

A numerical study of Gibbs u -measures for partially hyperbolic diffeomorphisms on \mathbb{T}^3 .

Andrey Gogolev, Itai Maimon and Aleksey N. Kolmogorov

ABSTRACT. We consider a hyperbolic automorphism $A: \mathbb{T}^3 \rightarrow \mathbb{T}^3$ of the 3-torus whose 2-dimensional unstable distribution splits into weak and strong unstable subbundles. We unfold A into two one-parameter families of Anosov diffeomorphisms — a conservative family and a dissipative one. For diffeomorphisms in these families we numerically calculate the strong unstable manifold of the fixed point. Our calculations strongly suggest that the strong unstable manifold is dense in \mathbb{T}^3 . Further, we calculate push-forwards of the Lebesgue measure on a local strong unstable manifold. These numeric data indicate that the sequence of push-forwards converges to the SRB measure.

1. Introduction

1.1. The setting. Consider the 3-dimensional torus $\mathbb{T}^3 = \mathbb{R}^3/\mathbb{Z}^3$ equipped with the standard (x, y, z) coordinates and a hyperbolic automorphism $A: \mathbb{T}^3 \rightarrow \mathbb{T}^3$ induced by the following integral matrix with determinant 1

$$A = \begin{pmatrix} 2 & 1 & 0 \\ 1 & 2 & 1 \\ 0 & 1 & 1 \end{pmatrix}$$

The eigenvalues of A are real and approximately equal to 0.20, 1.55 and 3.25. We denote the largest eigenvalue by λ , $\lambda \approx 3.25$, and corresponding eigenvector by v , $Av = \lambda v$,

$$v \approx \begin{pmatrix} 0.80 \\ 1.00 \\ 0.45 \end{pmatrix}$$

We will view A as a partially hyperbolic diffeomorphism whose center distribution is expanding. Further, we unfold A into two families of partially hyperbolic diffeomorphisms:

a *dissipative family*

$$f_{D,\varepsilon}(x, y, z) = (2x + y + \varepsilon \sin(2\pi x), x + 2y + z, y + z) \quad (1.1)$$

and a *conservative family*

$$f_{C,\varepsilon}(x, y, z) = (2x + y + \varepsilon \sin(2\pi x), x + 2y + z + \varepsilon \sin(2\pi x), y + z) \quad (1.2)$$

It is well-known that for small values of $\varepsilon > 0$ the diffeomorphisms $f_{*,\varepsilon}$, (here $*$ = D, C), remain Anosov, and also partially hyperbolic (with weakly expanding center distribution). Hence diffeomorphisms $f_{*,\varepsilon}$ leave invariant a one-dimensional strongly expanding foliation W_f^{uu} whose expansion rate is close to λ . Note that the point $p = (0, 0, 0)$ is fixed by all diffeomorphisms in the families.

1.2. Preview of the results and conjectures. We performed a very accurate (albeit non-rigorous) numerical calculations of the the finite-length strong unstable manifolds $W_{*,\varepsilon}^{uu}(p, R)$ which pass through p , up to length $R \approx 1.3 \cdot 10^8$. These numerical calculations strongly support the following conjecture.

CONJECTURE 1.1. *For all analytic diffeomorphisms f in a sufficiently small neighborhood of A the strong unstable foliation W_f^{uu} is transitive, i.e., it has a dense leaf.*

We actually expect the foliation W_f^{uu} to be minimal. However we did not calculate strong unstable leaves through non-periodic points because it is a much harder task. Figures 1.1 and 1.2 give a preview of our numerics in support of the above conjecture. These panels display first N intersection points of the strong unstable manifold $W^{uu}(p)$ with the 2-torus given by $y = 0$. We have calculated 10^8 intersection points. In the figures we only show up to 200,000 points because of large file size and because past 10^6 points one only sees Malevich's black square.

REMARK 1.2. In fact we show roughly $N/2$ points because we only display the points of intersection in the “one-half torus” given by $0 \leq z \leq 1/2$. We will display all our data on $[0, 1] \times [0, 1/2] \subset [0, 1] \times [0, 1] \simeq \mathbb{T}^2$ unless specified otherwise. Note that throughout the paper we maintain

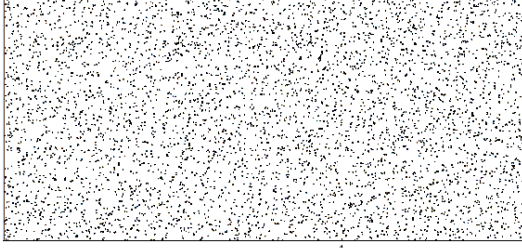
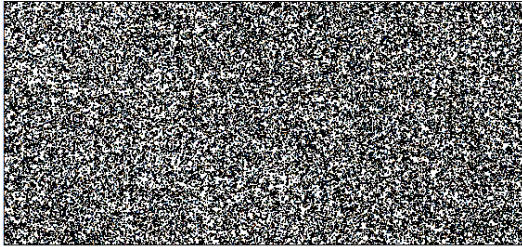
(a) u , conservative $\varepsilon=0.04$ $N=1 \times 10^4$ (b) u , conservative $\varepsilon=0.04$ $N=3 \times 10^4$ (c) u , conservative $\varepsilon=0.04$ $N=1 \times 10^5$

FIGURE 1.1. Intersection points of the strong unstable manifold and \mathbb{T}^2 transversal for f_C with $\varepsilon = 0.04$. The snapshots are shown for the first $N = 10,000, 30,000$ and $100,000$. The sequence of points appears to be dense providing support to Conjecture 1.1.

the convention to indicate the total number of points N in the captions to the figures. Hence, if readers counts the points on a figure then they would get approximately $N/2$ points. Displaying half of the torus helps to reduce file size. Also note that all diffeomorphisms $f_{*,\varepsilon}$ commute with the involution $i: (x, y, z) \mapsto (-x, -y, -z)$. It follows that the measures which we are interested in are invariant under i and all conditional measures on the \mathbb{T}^2 transversal are invariant under $(x, y) \mapsto (-x, -y)$.

In general, given a partially hyperbolic diffeomorphism $f: M \rightarrow M$, one reason to be interested in minimal sets of its strong unstable foliation W_f^{uu} is that minimal invariant sets support Gibbs u -measures associated to W_f^{uu} of Pesin and Sinai [PS83]. Gibbs u -measures are of great interest in

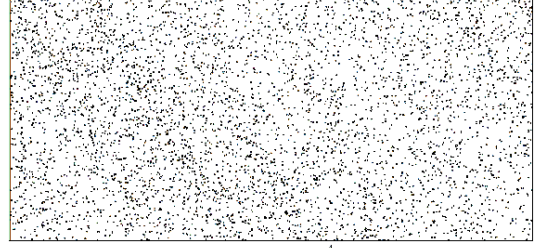
(a) u , dissipative $\varepsilon=0.04$ $N=1 \times 10^4$ (b) u , dissipative $\varepsilon=0.04$ $N=3 \times 10^4$ (c) u , dissipative $\varepsilon=0.04$ $N=1 \times 10^5$

FIGURE 1.2. Same as Figure 1.1 for f_D with $\varepsilon = 0.04$.

partially hyperbolic dynamics because they govern statistical properties of the dynamical system [Dol01, Dol04a]. Of course, in our setting the dynamical system is a transitive Anosov diffeomorphism which admits a unique SRB-measure and, hence, statistical properties are very well understood. However, perturbations of linear partially hyperbolic automorphisms are nice model examples where u -measures are not fully understood. We elaborate on our motivation to carry out the numerical study at the end of the introduction.

We view diffeomorphisms given by (1.1) and (1.2) as partially hyperbolic diffeomorphisms with one-dimensional strong unstable subbundles. Recall that a *Gibbs u -measure* of a partially hyperbolic diffeomorphism $f: M \rightarrow M$ is an f -invariant measure μ whose conditional measures on strong unstable plaques are absolutely continuous with respect to the induced Riemannian volume on strong unstable plaques. Gibbs u -measures were introduced by Pesin

and Sinai [PS83]¹ who also suggested a way to construct them as weak* partial limits of the sequence of averages

$$\bar{\nu}_K^{uu} \stackrel{\text{def}}{=} \frac{\nu^{uu} + f_*(\nu^{uu}) + \dots + f_*^{K-1}(\nu^{uu})}{K}, K \geq 1, \quad (1.3)$$

where ν^{uu} is a singular measure (on M) given by induced Riemannian volume on a strong unstable plaque. In our setting we can take ν^{uu} to be the singular measure (on M) given by the Lebesgue measure on a small plaque of $W^{uu}(p)$ with one end point being p . Hence we amend our calculation of $W^{uu}(p)$ with a numeric calculation of the strong unstable Jacobians of f^i , $i \leq K$, to obtain the averages numerically (more precisely, we look at the conditional measures of the averages on the 2-torus given by $y = 0$). Even though our evidence is not entirely conclusive we believe that the averages $\bar{\nu}_K^{uu}$ converge weakly. Further we calculate the SRB measure employing the zero-noise limit description of Young [You86]. The very different numeric procedures for calculating the u -measure and the SRB measure produce visually identical results for all values of ε as indicated on Figure 1.3. Hence we cautiously conjecture the following.

CONJECTURE 1.3. *For all analytic diffeomorphisms f in a sufficiently small neighborhood of A there exists a unique Gibbs u -measure (an f -invariant measure with absolutely continuous conditionals on strong unstable leaves) which then, of course, coincides with the SRB measure.*

This conjecture can be reformulated as follows: *for any analytic diffeomorphisms f in a sufficiently small neighborhood of A any f -invariant measure with absolutely continuous conditional measures on one-dimensional strong unstable plaques, in fact, has absolutely continuous conditional measures on two-dimensional unstable plaques.*

1.3. Motivation.

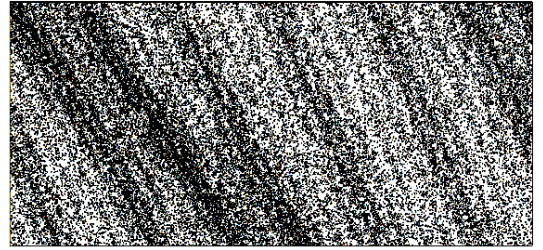
1.3.1. Our initial interest in transitivity (or minimality) question of the strong unstable foliation came from work on smooth conjugacy of higher dimensional Anosov diffeomorphisms [Gog08]. Transitivity of invariant expanding one-dimensional foliations (albeit not the strong unstable ones) played a key role in the arguments of [Gog08]. Families of diffeomorphisms in dimension three which we consider in this paper is the simplest setting where transitivity (minimality) is not understood.

We remark that minimality of the weak unstable foliation for $f_{*,\varepsilon}$ follows easily from structural stability. Indeed

¹Pesin and Sinai used a stronger definition which is equivalent to the one we give here, see [BDV00, Chapter 11].



(a) u , dissipative $\varepsilon=0.06$ $N=1 \times 10^5$



(b) SRB, dissipative $\varepsilon=0.06$ $N=1 \times 10^5$

FIGURE 1.3. Conditionals for u and SRB measure of f_D with $\varepsilon = 0.06$.

the conjugacy between A and f sends the weak unstable foliation W_A^{wu} to the weak unstable foliation W_f^{wu} of f . It is well known (see, e.g., [GG08]) that in general the conjugacy does not respect the strong unstable foliation. In fact, according to [RGZ17], the conjugacy respects strong unstable foliations if and only if the strong unstable and stable distributions of f integrate to an invariant foliation.

Note also that here we consider an irreducible automorphism A as a base-point for the families. The situation is quite different (but also poorly understood) in the case of reducible automorphisms. Indeed, for a reducible Anosov automorphism with weak-strong splitting in dimension 4 the closures of strong unstable leaves are 2-tori. And it is a very interesting question to investigate these closures and Gibbs u -measures for families which bifurcate into non-skew-product diffeomorphisms.

1.3.2. Minimality of strong unstable foliations of 3-dimensional partially hyperbolic diffeomorphisms was studied by Bonatti-Díaz-Ures [BDU02]. In particular, results of [BDU02] yield “large” C^1 -open sets of partially hyperbolic diffeomorphism with minimal strong stable and minimal strong unstable foliations. One of the crucial assumptions in the setting of [BDU02] is existence of hyperbolic periodic points of different indices (that is, a index 1 and index 2). The main technique of [BDU02] is construction of an invariant Morse-Smale section to the foliation. In our setting, when the center foliation is weakly expanding, this

technique is not applicable. Hence our setting can be considered as a complementary one to the setting of [BDU02].

Recall that homotopy class of $A: \mathbb{T}^3 \rightarrow \mathbb{T}^3$ contains the Mañé's example. This is a robustly transitive diffeomorphism $f_M: \mathbb{T}^3 \rightarrow \mathbb{T}^3$ which is partially hyperbolic but not Anosov [Mañ78]. To the best of our knowledge minimality of strong unstable foliation of f_M is also an open problem. Thus, understanding strong unstable foliation of perturbations of A and Mañé's example is a prerequisite for the following problem, which is a special case of Problem 1.6 in [BDU02].

PROBLEM 1.4. *Consider the space of robustly transitive partially hyperbolic diffeomorphisms $f: \mathbb{T}^3 \rightarrow \mathbb{T}^3$ which are homotopic to A , i.e., the induced map f_* on first homology group is given by A . Is strong unstable foliation W_f^{uu} minimal? Or at least transitive? If not, then is minimality (transitivity) of W_f^{uu} a C^1 -open and dense property in this space?*

Related to this problem, Potrie asked whether transitivity (or chain-recurrence) follows from partial hyperbolicity of $f: \mathbb{T}^3 \rightarrow \mathbb{T}^3$ in the homotopy class of A [Pot14]. Further, Potrie proved that there exists a unique quasi-attractor for each such f . Note that the attractor must be saturated by leaves of W_f^{uu} . Hence, minimality of W_f^{uu} would imply that the attractor is whole \mathbb{T}^3 .²

We also remark that robust minimality of strong unstable foliation was established in [PS83] under so called SH-condition. This condition does not hold in our setting. Finally, minimal sets of strong unstable foliation can be analyzed better in C^1 generic setting, see [CP15, Section 5.3].

1.3.3. It is interesting to understand the space of Gibbs u -measure $\text{Gibbs}^u(f)$, its dependence on the diffeomorphism and what bifurcations can occur. Note that it is known that $\text{Gibbs}^u(f)$ depends continuously on f in C^1 topology [Yan16] (see also [BDV00, Chapter 9]). Generalizing our numeric observation of uniqueness of the u measure we ask the following question.

PROBLEM 1.5. *Let $f: M \rightarrow M$ be a partially hyperbolic diffeomorphism of a 3-manifold M . Assume that f admits two distinct ergodic u -measures μ_1 and μ_2 . Is it true that*

$\text{supp}(\mu_1) \neq \text{supp}(\mu_2)$? *That is, do they necessarily have distinct supports?*³

1.4. Further discussion.

1.4.1. Our numerical evidence actually suggests that the push-forward measures $f_*^n \nu^{uu}$ converge to the SRB measure as $n \rightarrow \infty$. This was easier to detect than convergence of averages (1.3), which clearly converge slower. Note that convergence of $f_*^n \nu^{uu}$ to the unique Gibbs u -measure is a key assumption in the study of statistical properties of partially hyperbolic diffeomorphisms [Dol04a]. This assumption is difficult to verify theoretically when dynamics along the center subbundle is non-linear.⁴

1.4.2. Another observation is that our numerical experiments suggest that the u -measure coming from the strong unstable leaf through p agrees with the SRB measure well beyond the range of small ε . (The splitting at p survives for all $\varepsilon > 0$.) This is indicated on Figure 1.4. At $\varepsilon = \frac{1}{2\pi} \approx 0.159$ bifurcation from diffeomorphisms to non-invertible maps occurs and the “folding” which happens beyond this parameter value is clearly visible on Figure 1.4. Note that pictures of u and SRB measures do not give any indication if the bifurcation from partially hyperbolic (or Anosov) world happens. Indeed, it is actually very plausible that prior to the critical value $\frac{1}{2\pi}$ no such bifurcations happen; that is, $f_{D,\varepsilon}$ stays Anosov with weak-strong unstable splitting for $\varepsilon < \frac{1}{2\pi}$.

To provide some support we numerically calculate points of period 3 and corresponding eigenvalues using the following procedure. We consider a dense $2,000 \times 2,000 \times 2,000$ mesh of points (x_i, y_j, z_k) and apply dynamics 3 times to obtain the final point $f^3(x_i, y_j, z_k)$. If for some (i, j, k) the starting and final points end up within $D = D(x_i, y_j, z_k) < 0.02$ we adjust the coordinates (x_i, y_j, z_k) coordinates to minimize the Euclidean distance with a gradient descent method. The partial derivatives $(\frac{\partial D}{\partial x}, \frac{\partial D}{\partial y}, \frac{\partial D}{\partial z})$ at (x_i, y_j, z_k) are calculated numerically. Once $D < 10^{-5}$, we find the cubic roots of eigenvalues of $Df^3(x_i, y_j, z_k)$.

This numerics gives 16 distinct eigenvalue graphs. And this is consistent with the Lefschetz formula which yields 91 points fixed by $f_{*,\varepsilon}^3$. One of these points is the fixed

²The first author believes that non-trivial trapping regions exist for some point-wise partially hyperbolic $f: \mathbb{T}^3 \rightarrow \mathbb{T}^3$ in the homotopy class of A . If so, it would be interesting to investigate the structure of W_f^{uu} and how the bifurcation happens.

³It was suggested to us by Dmitry Dolgopyat that this question also makes sense in higher dimensions if one additionally assumes that f is accessible (or considers u -measures supported on an accessibility class).

⁴However, for transitive Anosov diffeomorphisms mixing implies that $f_*^n \nu^u$ converges to the SRB measure, where ν^u is Lebesgue measure on an unstable plaque. This was explained to us by F. Rodriguez Hertz.

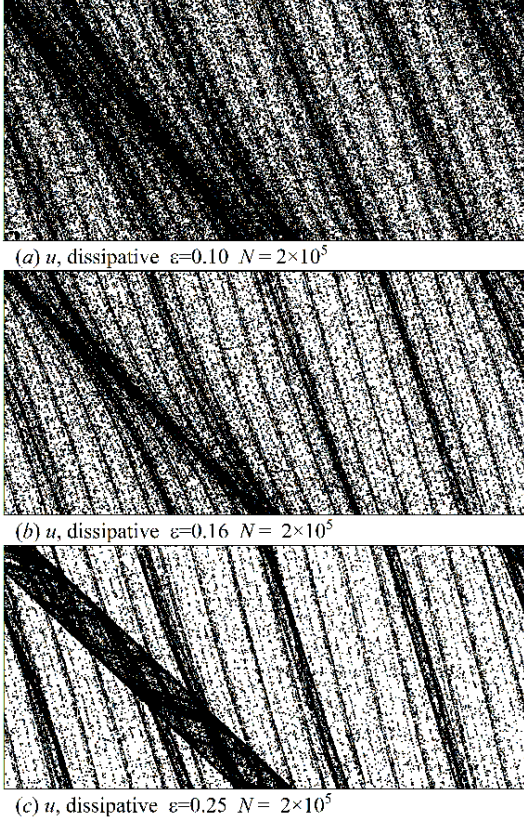


FIGURE 1.4. Conditionals of the u -measure on \mathbb{T}^2 in the dissipative family f_D .

point p . The rest give 30 orbits of period 3 none of which is fixed by the involution i . Hence the involution breaks up these orbits into 15 pairs with identical eigenvalue data. Figure 1.5 displays dependence of the eigenvalue data on ε . We observe clear separation of the spectrum into three bands for both conservative and dissipative ($\varepsilon < \frac{1}{2\pi}$) families.

1.4.3. Ruelle provided a formula for the derivative of the SRB measure with respect to the diffeomorphism (Anosov, or more generally on a hyperbolic attractor) [Rue97], see also [Rue98, Jia12]. If we denote by μ_ε the SRB measure of $f_{D,\varepsilon}$ and expand with respect to ε

$$\mu_\varepsilon = \mu_0 + \varepsilon \delta\mu + \text{h.o.t.}$$

Then, according to Ruelle's formula,

$$\delta\mu(\Phi) = \sum_{n \geq 0} \int \langle \nabla(\Phi \circ A^n, X) \rangle d\mu$$

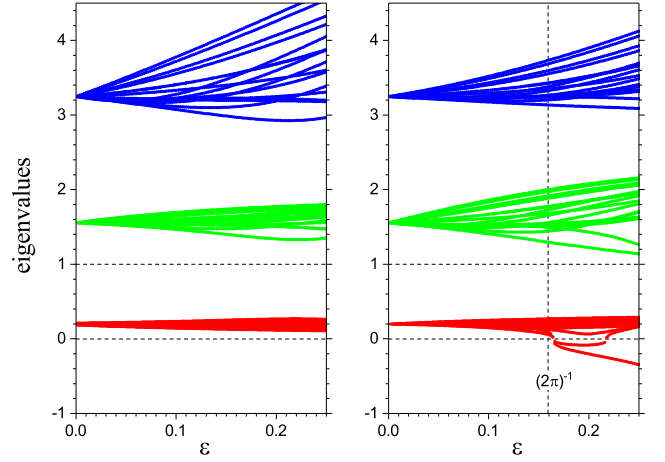


FIGURE 1.5. Spectrum at the fixed point and 15 orbits of period 3. Note that it is disjoint with horizontal line 1 and is confined to three disjoint bands, suggesting that diffeomorphisms f_C (left panel) and f_D (right panel) stay Anosov with weak-strong unstable splitting.

where $\Phi \in C^\infty(M, \mathbb{R})$ and X is the vector field $\partial f_{D,\varepsilon} / \partial \varepsilon|_{\varepsilon=0}$. Similar formula for u -measure of a partially hyperbolic diffeomorphism (more specifically, an element of an Anosov action) was established by Dolgopyat [Dol04b]. Remarkably, the formula of Dolgopyat holds for families f_ε even when the uniqueness of u -measure is not known for $\varepsilon > 0$. That is, all families of u -measures which start at μ_0 have the same derivative. Thus, even though results of Dolgopyat are not directly applicable in our setting, we are less confident about Conjecture 1.3. One should exercise caution when perusing our numeric evidence for Conjecture 1.3 as it might be missing some higher order phenomena.

2. Background

In this section we briefly summarize the needed background. For in depth discussions of partial hyperbolicity, SRB measures and Gibbs u -measures we refer the reader to [Pes04, BDV00, You02, PS83, Dol01].

2.1. Anosov and partially hyperbolic diffeomorphisms. Recall that a self-diffeomorphism $f: M \rightarrow M$ of a compact Riemannian manifold is called *Anosov* if the tangent space $T_x M$ at every $x \in M$ is split into Df -invariant subbundles, $T_x M = E^s(x) \oplus E^u(x)$, and $Df|_{E^s}$ is uniformly expanding while $Df|_{E^u}$ is uniformly contracting.

An important generalization is the concept of *partially hyperbolic diffeomorphism* $f: M \rightarrow M$ which assumes existence of a Df -invariant splitting $T_x M = E^{ss}(x) \oplus E^c(x) \oplus E^{uu}(x)$, where $Df|_{E^{ss}}$ is uniformly expanding, $Df|_{E^{uu}}$ is uniformly contracting and $Df|_{E^c}$ has intermediate growth, that is,

$$\|Df|_{E^c}\| \cdot \|(Df|_{E^{uu}})^{-1}\| < 1,$$

and

$$\|Df|_{E^{ss}}\| \cdot \|(Df|_{E^c})^{-1}\| < 1$$

It is well-known that E^{ss} and E^{uu} integrate to foliations which we denote by W^{ss} and W^{uu} , respectively.

For sufficiently small $\varepsilon > 0$ the diffeomorphisms $f_{*,\varepsilon}$ given by (1.1) and (1.2) are Anosov with 2-dimensional unstable distributions. However, because A has real spectrum $\lambda_1 < 1 < \lambda_2 < \lambda_3$, the unstable distribution admits a finer invariant splitting $E^c \oplus E^{uu}$ and, hence, $f_{*,\varepsilon}$ can also be viewed as a partially hyperbolic diffeomorphism.

2.2. SRB measures. Informally speaking, SRB⁵ measures are invariant measures which are most compatible with volume when volume itself is not invariant. More precisely, consider a self-diffeomorphism $f: M \rightarrow M$, then an invariant measure μ is called an *SRB measure* (or a *physical measure*) if its basin of attraction has positive volume; that is, the set of points $x \in M$ such that

$$\forall \varphi \in C^0(M) \quad \lim_{n \rightarrow \infty} \frac{1}{n} \sum_{i=0}^{n-1} \varphi(f^i x) = \int_M \varphi d\mu$$

has positive volume. For transitive Anosov diffeomorphisms the SRB measure μ is unique and is well-understood by work of Sinai, Ruelle and Bowen. It can be characterized by the following equivalent conditions.

- (C1) μ has absolutely continuous conditionals on unstable plaques;
- (C2) μ is the zero-noise limit of small random perturbations of f .

Our numeric calculations of the SRB measure for $f_{*,\varepsilon}$ will rely on the second characterization which is due to L.-S. Young [You86]. We will elaborate on it later in Section 3.2.

2.3. Gibbs u -measures. The definition of Gibbs u -measures for partially hyperbolic diffeomorphisms comes from postulating characterization (C1) above. Given a partially hyperbolic diffeomorphism $f: M \rightarrow M$, an invariant measure μ is called a *Gibbs u -measure* if it has absolutely

continuous conditionals on unstable plaques. Then the density of the conditional measure on a plaque $W_f^{uu}(x, R)$ is given by

$$\rho_x^{uu}(y) = \prod_{i \geq 0} \frac{Jac(f^{-1}|_{E^{uu}(f^{-i}(y))})}{Jac(f^{-1}|_{E^{uu}(f^{-i}(x))})}, \quad y \in W_f^{uu}(x, R) \quad (2.4)$$

Note that in our setting the SRB measure is automatically a u -measure. In general, of course, the converse does not hold. Still, under additional assumptions this could be the case. For example, Bonatti and Viana showed that if E^c is mostly contracting then there are finitely many ergodic Gibbs u -measures which are the SRB measures [BV00].

Dolgopyat, assuming uniqueness of the u -measure and that push-forwards $f_*^n \nu^{uu}$, $n \geq 0$, converge to the u -measure, established various limit theorems previously known in the Anosov setting [Dol04a].

2.4. Numerics. We have chosen the C language to implement the numerical algorithms for computing orbits, u -measures, and SRB-measures in this study. Due to the high precision requirements in the calculation of u - and SRB-measures, we employed quadmath library available in gcc 4.4.6. The quadruple precision `_float128` type provides machine epsilon $2^{-112} \approx 10^{-34}$. We relied on the Box-Muller transformation [BM58] of random numbers produced with a linear congruential generator [PM88] to introduce Gaussian noise in the SRB calculations. Generation of u -measures proved to be the most expensive part of this numerical study but the computational cost was fairly low, at about 1,000 CPU hours per 10^8 points.

3. The results

3.1. Numerics for the strong unstable manifold.

Let $f: \mathbb{T}^3 \rightarrow \mathbb{T}^3$ be a partially hyperbolic diffeomorphism which belongs to the family (1.1) or the family (1.2) for small $\varepsilon > 0$. Here we explain numerics for the strong unstable manifold $W_f^{uu}(p)$ and present the numerical evidence supporting Conjecture 1.1 using Figures 3.2 and 3.3.

Consider the universal cover $\mathbb{R}^3 \simeq \{(x, y, z)\}$. Denote by $\tilde{f}: \mathbb{R}^3 \rightarrow \mathbb{R}^3$ the lift of f that fixes point $(0, 0, 0)$, which we still denote by p . Also denote by $\tilde{W}_f^{uu}(p)$ the connected component of the lift of $W_f^{uu}(p)$ which contains p . Then the strong unstable manifold $\tilde{W}_f^{uu}(p)$ can be viewed as a graph of a function φ^{uu} defined on the y -axis

$$\varphi^{uu}: \mathbb{R} \rightarrow \mathbb{R}^2, \quad y \mapsto (x_y, z_y) \stackrel{\text{def}}{=} \varphi^{uu}(y)$$

as shown on Figure 3.1. For each integer y_0 the point (x_{y_0}, z_{y_0}) is the intersection point of the plane $\mathbb{R}^2 \simeq \{y =$

⁵Sinai-Ruelle-Bowen.

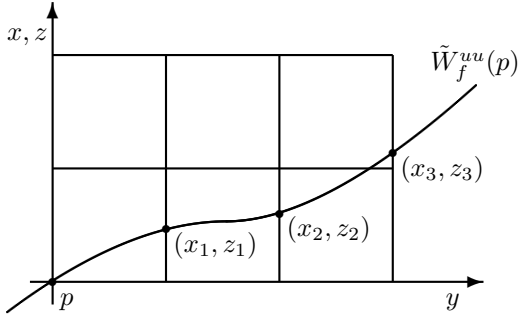


FIGURE 3.1. The lift of the strong unstable manifold and the sequence of points $\{(x_{y_0}, z_{y_0}); y_0 \geq 1\}$.

$y_0\}$ and $\tilde{W}_f^{uu}(p)$ and the point

$$(x_{y_0}, z_{y_0}) \mod \mathbb{Z}^2$$

is an intersection point of the 2-torus $\mathbb{T}^2 \simeq \{y = 0\}$ and $W_f^{uu}(p)$.

To calculate (x_{y_0}, z_{y_0}) we carry out the following procedure. Denote by v_p the vector tangent to $\tilde{W}_f^{uu}(p)$ at p (which is an eigenvector of $D_p \tilde{f}$). And let cv_p be a vector proportional to v_p whose y -coordinate equals to y_0 . Also let λ_p be the corresponding eigenvalue, $D_p \tilde{f} v_p = \lambda_p v_p$. Then to calculate the point $q = (x_{y_0}, y_0, z_{y_0}) \in \tilde{W}_f^{uu}(p)$ we employ the following iterative algorithm. First we let q_{-50}^1 be the end point of scaled eigenvector $\frac{c}{\lambda_p^{50}} v_p$. We calculate the first approximation by using the dynamics

$$q^1 = \tilde{f}^{50}(q_{-50}^1).$$

Then we look at the y -coordinate of q^1 , compare it to y_0 , use a linear mixing scheme with parameter 0.1 to adjust the initial point q_{-50}^1 along v_p to a new initial point q_{-50}^2 , and repeat the procedure $n = 1,000 - 2,000$ times to achieve convergence of q^n to the desired $q \in \tilde{W}_f^{uu}(p)$ within $10^{-24} y_0$ from the plane $\{y = y_0\}$.

By repeating this iterative calculation we obtain the sequence of intersection points of $W_f^{uu}(p)$ and $\mathbb{T}^2 \simeq \{y = 0\}$

$$\{(x_{y_0}, z_{y_0}); y_0 \geq 1\}$$

We calculate up to 10^8 points in this sequence. The images we obtain clearly indicate that points cluster more for larger values of ε . Still the sequence does not seem to leave any gaps in \mathbb{T}^2 . This supports our density conjecture as shown on Figures 3.2 and 3.3 where as we “zoom in” at

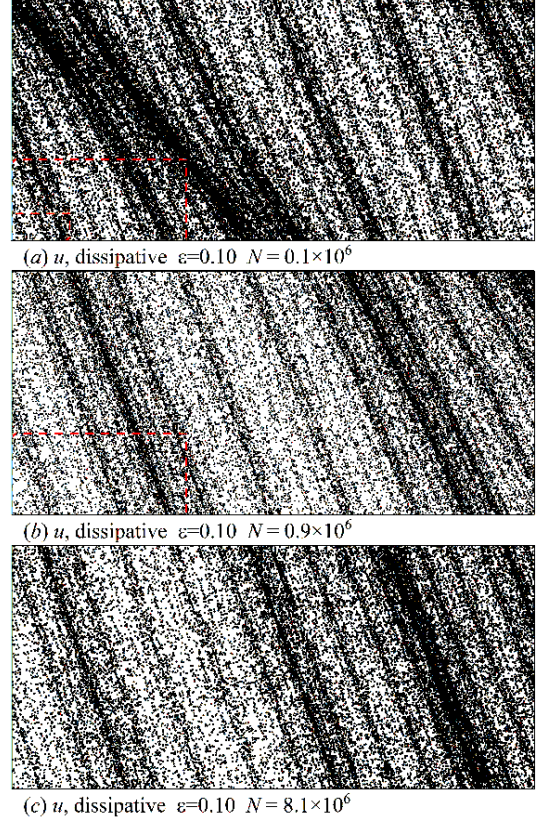


FIGURE 3.2. Support for Conjecture 1.1. The intersection points are plotted for f_D with $\varepsilon = 0.1$. Two lower panels are $\times 3$ and $\times 9$ zoom-ins. The number of points is increased proportionally to the area of the domain.

point p . Zooming in does not reveal any regions free of intersection points. For the conservative family, points tend to cluster much less and distribute more evenly. We include the figures for the dissipative family only since they are more interesting.

3.1.1. Reliability of numerics. The numerical data for the sequence of points $\{(x_{y_0}, z_{y_0}); y_0 \geq 1\}$ is the key data providing support to our conjectures. Thus we briefly elaborate on the reliability of our calculations.

The iterative calculation of points $q = (x_{y_0}, y_0, z_{y_0})$ has two sources of numerical errors. The first one is algorithmic and is associated with the deviation of q_{-K} ($K = 50$) from the strong unstable manifold $\tilde{W}_f^{uu}(p)$ and can be estimated as follows. Recall that q is obtained as $\tilde{f}^K(q_{-K})$, where q_{-K} is first guessed as $\lambda_p^{-K} v_p$. Figure 3.4 shows

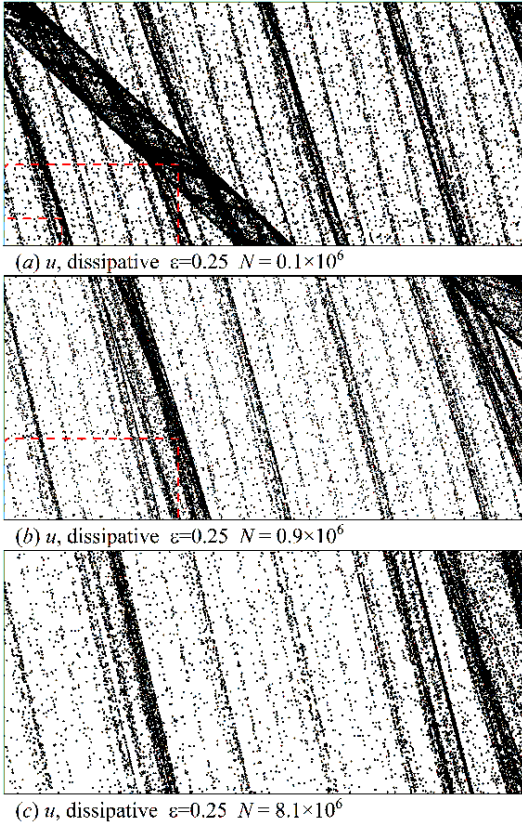


FIGURE 3.3. Support for Conjecture 1.1. Same as in Figure 3.2 but for $\varepsilon = 0.25$.

that, once converged, $q_{-K} = cv_p$ remains within a factor of 10 from the original guess for all $1 \leq y_0 \leq 10^8$. The value of c does not exceed 10^{-17} for the considered $\lambda_p \geq 3.25$ corresponding to $\varepsilon = 0.1$. Since the strong unstable manifold and the line spanned by v_p have quadratic tangency at small values of c , the transverse distance from q_{-K} to $\tilde{W}_f^{uu}(p)$ is of the order c^2 . Over the K steps, the error in the determination of the intersection of the strong unstable manifold and \mathbb{T}^2 transversal is amplified by a factor of λ_\perp^K . According to Figure 1.5, λ_\perp along the weak unstable direction is below 2 for $\varepsilon \leq 0.1$. Hence, the resulting error does not exceed $10^{-34} \times 2^{50} < 10^{-18}$.

The second source of error is the accumulation of rounding errors due to machine precision. The resulting accuracy depends on the particular set of performed operations and is not easy to evaluate. In order to examine the sensitivity of our results to machine precision, we compare the errors

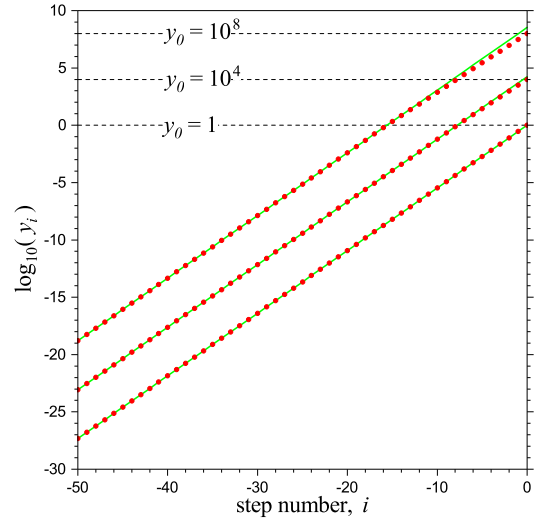


FIGURE 3.4. Converged sequences of y_i ($-K \leq i \leq 0$, $K = 50$) for several target y_0 values in the dissipative family with $\varepsilon = 0.1$. Points with $y_i \ll 1$ are essentially scaled along the v_p eigenvector by λ_p .

in determining q for the full range of y_0 using single, double, and quadruple precisions. The machine epsilons corresponding to the float, double, and `_float128` data types are $2^{-23} \approx 10^{-7}$, $2^{-52} \approx 10^{-16}$, and $2^{-112} \approx 10^{-34}$, respectively. Figure 3.5(a) shows how far q points calculated with single or double precisions deviate from those calculated with the quadruple precision. One can see that the use of double instead of float reduces the error for all considered y_0 by about 10^{-9} which is consistent with the difference in the machine epsilons for the two data types. Based on this observation, we expect that the use of `_float128` instead of double reduces the error by an additional factor of about 10^{-18} and the rounding error should not exceed 10^{-25} for y_0 up to 10^8 .

The relative magnitude of the two errors can be controlled by the choice of K : the algorithmic error decreases with K roughly as $(\lambda_p^{min})^{-2K} \times (\lambda_\perp^{max})^K$ and the rounding error grows with K . Our final test results plotted in Figure 3.5(b) illustrate that the chosen value of $K = 50$ ensures sufficient numerical accuracy to achieve iterative convergence of the q point positions in the intersecting plane within $10^{-24}y_0$. Indeed, the distance between q calculated for $K = 50$ and those calculated at smaller K values drops below 10^{-22} by $K = 35$ for all considered y_0 values.

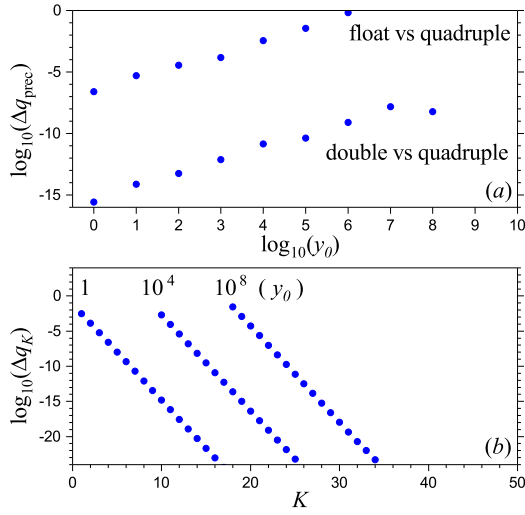


FIGURE 3.5. Analysis of numerical errors in the determination of q for the dissipative family and $\varepsilon = 0.1$. (a) The effect of machine precision on the accumulation of rounding errors for $K = 50$. Δq_{prec} is the Euclidian distance between q points calculated with quadruple precision and with either double or single precision. (b) Convergence of q points as a function of the number of steps K . Δq_K is the Euclidian distance between q points calculated at $K = 50$ and lower K values.

We conclude that both sources of numeric error are negligible (10^{-18} and 10^{-25}) than compared to our stopping criterion $10^{-24}y_0 \leq 10^{-16}$. Note that even though $10^{-24}y_0$ is deviation from the intersecting plane it also gives an error of the same magnitude within the plane because the strong unstable manifold intersects the plane with an angle, hence, the error projects to the plane. Therefore, the settings used in this computational study allow us to resolve the point positions better than 10^{-16} for y_0 up to 10^8 and the procedure can be used (by further lowering the iteration stopping parameter below $10^{-24}y_0$) to generate points with much larger y_0 values.

3.2. Numerics for SRB measures. We recall the description of SRB measure as zero-noise limit by L.-S. Young [You86]. The idea is to approximate a diffeomorphism $f: M \rightarrow M$ by random Markov chains. To define the Markov chain consider Borel probability measures $p(\cdot|x)$ for all $x \in M$. Given a Borel set $A \subset M$ one can think about

$p(A|x)$ as the probability of sending x to the set A . A measure μ on M is *stationary* if

$$\mu(A) = \int_M p(A|x) d\mu(x)$$

for every Borel set A .

A *small random perturbation* of $f: M \rightarrow M$ is a one parameter family of Markov chains given by transition probabilities $p^\sigma(\cdot|x)$, $x \in M$, which satisfy $p^\sigma(\cdot|x) \rightarrow \delta_{f(x)}$ as $\sigma \rightarrow 0$ uniformly in $x \in M$. (We will think of σ as a discrete parameter.) The following properties were established in [You86].

1. If $x \mapsto p(\cdot|x)$ is continuous then a stationary measure exists;
2. If $p(\cdot|x)$ are absolutely continuous with respect to volume for all $x \in M$ then the stationary measure is also absolutely continuous;
3. If $\{p^\sigma(\cdot|x)\}$ is a small random perturbation of a diffeomorphism f , then all limit points of a sequence of stationary measures $\{\mu^\sigma\}$, as $\sigma \rightarrow 0$, are f -invariant.

Given a measure ν on a set of diffeomorphisms $\Omega \subset \text{Diff}(M)$ one can define the transition probabilities by

$$p(A|x) = \nu\{g : g(x) \in A\}. \quad (3.5)$$

Now, if $\nu^\sigma \rightarrow \delta_f$ as $\sigma \rightarrow 0$ then corresponding Markov chains $\{p^\sigma(\cdot|x)\}$ yield a small random perturbation of f .

Theoretical support for our computations of SRB measures which we are about to describe comes from the following theorem (which is a particular case of a more general result in [You86]).

THEOREM 3.1 ([You86]). *Let $f: M \rightarrow M$ be a transitive Anosov diffeomorphism. There exists a C^1 small and C^2 -bounded neighborhood $\Omega \ni f$ such that if $\{\nu^\sigma\}$ are Borel probability measures on Ω with $\nu^\sigma \rightarrow \delta_f$, $\sigma \rightarrow 0$, and corresponding transition probabilities $\{p^\sigma(\cdot|x)\}$ given by (3.5) are absolutely continuous then (every) sequence of stationary measures μ^σ converges to the SRB measure.*

Hence this theorem gives a lot of credibility to numerical calculations where one applies dynamics and small random noise at each step to obtain an approximation for the SRB measure. More precisely we consider a sequence of symmetric Gaussians ξ^σ on \mathbb{R}^3 with zero mean and standard deviation σ . Then $\xi \rightarrow \delta_{(0,0,0)}$ as $\sigma \rightarrow 0$. We define

$$\nu^\sigma = f + (\xi^\sigma \bmod \mathbb{Z}^3)$$

that is, we post-compose our dynamics with a small random translation on \mathbb{T}^3 . Then, clearly, $\nu^\sigma \rightarrow \delta_f$ as $\sigma \rightarrow 0$ and one

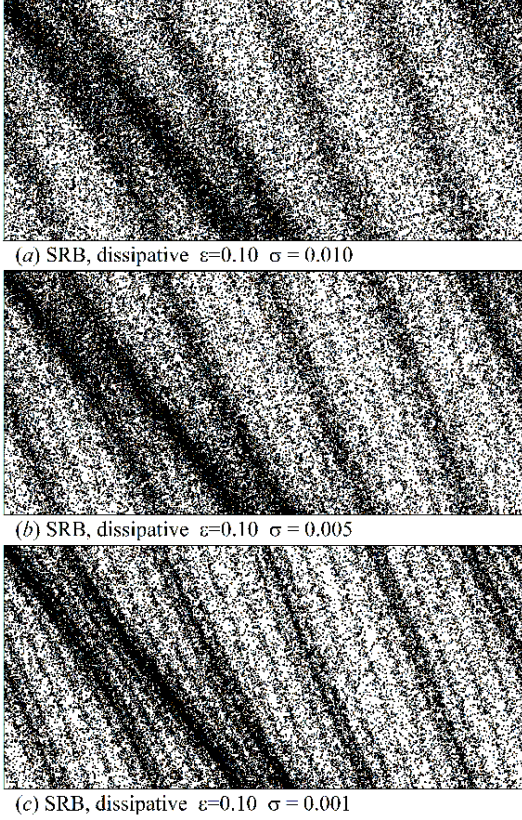


FIGURE 3.6. Approximations of the SRB measure of f_D with $\varepsilon = 0.1$ as $\sigma \rightarrow 0$.

easily sees that the transition probabilities are absolutely continuous. Hence the theorem above applies. (Technically, we also need to truncate Gaussians to ensure C^1 -smallness of the perturbation, but practically this makes no difference as we are interested in very small σ .)

The numeric scheme is as follows. We begin with a random point q_0 on \mathbb{T}^3 and generate a σ -approximation of the SRB measure by consecutive application of f and addition of Gaussian noise ξ^σ . That is,

$$q_{i+1} = f(q_i) + \xi^\sigma$$

Note that we only work in the parameter range $\sigma \gg 10^{-32}$ so that the numeric error in calculation of f is much smaller than the (small) random noise. Therefore, exponential accumulation of the numeric error is not of any concern. On Figure 3.6 we display several approximations for different values of σ . For all further SRB measures numerics, which

we need for comparisons with u -measures numerics, we use $\sigma = 10^{-29}$.

3.3. Comparing Gibbs u and SRB measures. Consider the averaged Dirac measures

$$\Sigma^u = \frac{1}{N} \sum_{y_0=1}^N \delta_{(x_{y_0}, z_{y_0})} \quad (3.6)$$

corresponding to the u -measure, and

$$\Sigma^{\text{SRB}} = \frac{1}{N} \sum_{q_i \in S} \delta_{q_i} \quad (3.7)$$

corresponding to the SRB measure, where S is the slice $\{(x, y, z \in \mathbb{T}^3 : -0.005 \leq y \leq 0.005\}$ which contains N points. For the dissipative family point distributions Σ^u and Σ^{SRB} visually coincide for all parameters in our range $\varepsilon \in [0, 0.25]$ (see Figure 1.3). On the other hand, for the conservative family, the SRB measure is the uniform Lebesgue measure as it supposed to be, while the u -measure appears to be an absolutely continuous measure with a non-constant density, as one can see on the top panel of Figure 3.7. The “non-uniformity” increases as we increase ε . The explanation for this discrepancy is that (3.7) gives the (approximation of) true conditional measure on \mathbb{T}^2 of the SRB measure, while (3.6) does not give (an approximation of) the conditional of $f_*^n \nu^{uu}$. Hence we proceed with the numeric calculation of the true conditional of $f_*^n \nu^{uu}$ on \mathbb{T}^2 and present the numeric evidence that the measures indeed coincide.

REMARK 3.2. Note however that the conditional of $f_*^n \nu^{uu}$ on \mathbb{T}^2 is absolutely continuous with respect to (3.6). Hence, if Σ^u converges to an absolutely continuous measure (which we numerically verified by using histograms) then $f_*^n \nu^{uu}$ converges to an absolutely continuous measure on \mathbb{T}^3 as $n \rightarrow \infty$. And, since this measure is invariant, it must be the volume. In view of this remark our further numeric verification of convergence of $f_*^n \nu^{uu}$ to volume becomes somewhat redundant. However we still find it important to have direct numeric evidence.

REMARK 3.3. By analyzing distribution functions of the Dirac averages (3.6) and (3.7) in the dissipative family we can also very clearly conclude that Σ^u and Σ^{SRB} do not converge to the same measure on \mathbb{T}^2 . Hence, as to be expected, the above discussion also applies to the dissipative family. However visually the point distributions Σ^u and Σ^{SRB} are identical in this case. This happens because for

singular measures, when looking at the pictures of approximating point distributions we can only see the measure class rather than the measure itself.

3.4. The conditional measure on $\mathbb{T}^2 \simeq \{y = 0\}$ for Gibbs u -measure. Now we explain precisely our numerics for the conditional of the Gibbs u -measure. Let $r \in \tilde{W}_f^{uu}(p)$ be a point very close to p . Consider the Lebesgue measure on $\tilde{W}_f^{uu}(p)$ induced by the canonical flat Riemannian metric on \mathbb{R}^3 . And denote by ν^{uu} the normalized Lebesgue measure supported on the strong unstable plaque $[p, r]^{uu} \subset \tilde{W}_f^{uu}(p)$. Then, by using calculus, the density of $f_*^n \nu^{uu}$ with respect to the Lebesgue measure on $\tilde{W}_f^{uu}(p)$ is given by

$$\rho(q) = \text{Jac}(f^{-n}|_{E^{uu}(q)}), \quad q \in [p, f^n(r)]^{uu}$$

This Jacobian density can be easily evaluated numerically because, as we explained in Section 3.1, we can accurately calculate points q on $\tilde{W}_f^{uu}(p)$ together with their preimages under f^{-n} , $n \leq 50$. Hence to find $\rho(q)$ approximately we look at points $q - \Delta q, q + \Delta q$ on $\tilde{W}_f^{uu}(p)$ and their preimages; and then evaluate the Jacobian numerically by taking the ratio.⁶

Recall that we need to further take the conditional measure of $f_*^n \nu^{uu}$ on $\mathbb{T}^2 \simeq \{y = 0\}$. Then, one can easily see (for example, by taking the limit as the width of the \mathbb{T}^2 -slice goes to zero) that the expression for the conditional measure at the intersection point (x_{y_0}, y_0, z_{y_0}) , $y_0 \in \mathbb{Z}_+$, depends on the angle between $\tilde{W}_f^{uu}(p)$ and \mathbb{T}^2 at (x_{y_0}, y_0, z_{y_0}) . Namely, one has the following formula for the conditional of $f_*^n \nu^{uu}$ on $\mathbb{T}^2 \simeq \{y = 0\}$

$$\Sigma_{\rho a}^u = \frac{1}{W(N)} \sum_{y_0=1}^N \rho(x_{y_0}, y_0, z_{y_0}) a(x_{y_0}, z_{y_0}) \delta_{(x_{y_0}, z_{y_0})},$$

where ρ was defined above,

$$W(N) = \sum_{y_0=1}^N \rho(x_{y_0}, z_{y_0}) a(x_{y_0}, y_0, z_{y_0});$$

and the “angle weight” is defined by

$$a(x_{y_0}, z_{y_0}) = \frac{1}{\langle v^\perp, v^{uu} \rangle},$$

where v^\perp is unit vector at (x_{y_0}, y_0, z_{y_0}) perpendicular to \mathbb{T}^2 and v^{uu} is the unit vector at (x_{y_0}, y_0, z_{y_0}) tangent to

⁶We use $\|\Delta q\| = 10^{-7}$. With such step size, tests similar to ones in subsection 3.1.1 give an upper bound of 10^{-6} on the precision for weight values.

$\tilde{W}_f^{uu}(p)$. Again, coefficient a is easy to calculate since we can numerically calculate the tangent vectors v^{uu} .

The density weights ρ and a have different genesis. Hence, for the purpose of analyzing $\Sigma_{\rho a}^u$ we also introduce the “component” Dirac averages

$$\Sigma_\rho^u = \frac{1}{W} \sum_{y_0=1}^N \rho(x_{y_0}, y_0, z_{y_0}) \delta_{(x_{y_0}, z_{y_0})},$$

and

$$\Sigma_a^u = \frac{1}{W} \sum_{y_0=1}^N a(x_{y_0}, z_{y_0}) \delta_{(x_{y_0}, z_{y_0})},$$

which are normalized by the corresponding total weight W .

3.5. Comparing Gibbs u and SRB measures numerically. Our calculations of ρ , a and point distributions Σ^u , Σ_ρ^u , Σ_a^u and $\Sigma_{\rho a}^u$ are summarized on Figures 3.7, 3.8 and 3.9.

On Figure 3.7 the values of weights are coded in color. The average value is normalized to equal 1. By the definition the “angle weight” $a = a(x_{y_0}, z_{y_0})$ is a continuous function on \mathbb{T}^2 . Notice that a (middle panel) varies only slightly, within 2% of the average. On the other hand, on the bottom panel shows that ρ varies a lot. Further, the graph of $\rho = \rho(x_{y_0}, y_0, z_{y_0}) = \rho(y_0)$ given on Figure 3.8 shows that ρ is unbounded (that is, if normalize ρ so that $\rho(0) = 1$ then ρ is unbounded function of y_0) and have certain “self-similar” structure.

By examining Figure 3.7 one can see that ρ smoothes out the point distribution Σ^u , that is, it makes Σ_ρ^u more uniform than Σ^u . Curiously, and we have no good explanation for this, the “angle weight” a makes point distribution less uniform, but, as we remarked before, a has a very small effect on the distribution.

In order to quantify these observations coming from Figure 3.7 we use a 200×200 square grid to partition \mathbb{T}^2 into 40,000 bins. For each bin \mathcal{B} we calculate its total weight

$$w^u(\mathcal{B}) = \#\{y_0 \leq N : (x_{y_0}, z_{y_0}) \in \mathcal{B}\}$$

as well as the weight adjusted by ρ

$$w_\rho^u(\mathcal{B}) = \sum_{\substack{y_0=1, \\ (x_{y_0}, z_{y_0}) \in \mathcal{B}}}^N \rho(y_0).$$

And weights $w^{\text{SRB}}(\mathcal{B})$, $w_a^u(\mathcal{B})$ and $w_\rho^u(\mathcal{B})$ are defined analogously. Further we calculate relative standard deviation

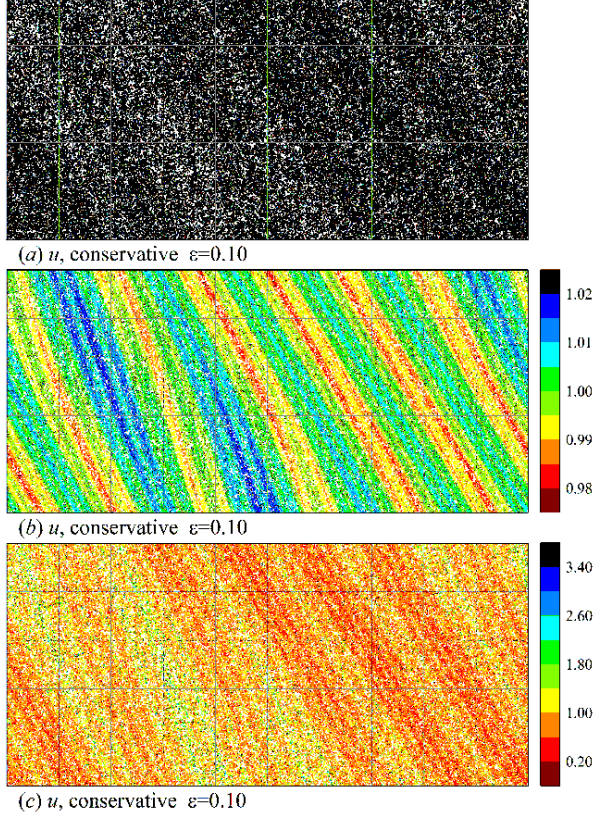


FIGURE 3.7. Dirac averages Σ^u , Σ_a^u and Σ_ρ^u , $N = 200,000$. The weights in lower panels are needed for proper scaling of the distribution in the top panel in order to obtain (the approximation of) the conditional measure on the transversal. Note that, for example, in right lower corner point Σ^u takes large values, a is above average, and ρ takes small values.

in order to have a single number which measures closeness to the uniform distribution

$$RSD^u = \frac{1}{\bar{w}^u} \left(\frac{1}{40,000} \sum_{\mathcal{B}} (w^u(\mathcal{B}) - \bar{w}^u)^2 \right)^{\frac{1}{2}},$$

where \bar{w}^u is the average of the weights. Analogously we have relative standard deviations RSD^{SRB} , RSD_ρ^u , RSD_a^u and $RSD_{\rho a}^u$. The dependence of relative standard deviations on the number of points in the range $N = 10^6, \dots, 10^8$ is shown on Figure 3.9. Indeed, we see that RSD^{SRB} , RSD_ρ^u and $RSD_{\rho a}^u$ decay to zero roughly proportionally to $\frac{1}{\sqrt{N}}$. Unfortunately we cannot differentiate between RSD_ρ^u and $RSD_{\rho a}^u$.

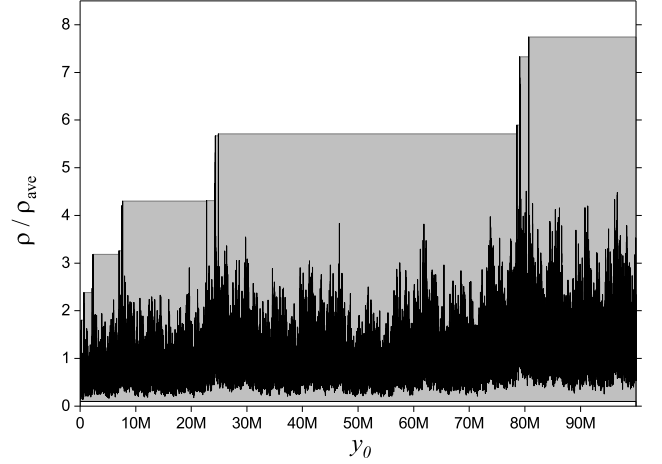


FIGURE 3.8. Dependence of ρ/ρ_{ave} on y_0 for u -measure of $f_{C,\varepsilon=0.1}$. Values of ρ_{ave} is calculated over the full range of $N = 10^8$ points. The minimum 0.1245 is achieved at 1. The height of the shaded area increases with y_0 whenever ρ/ρ_{ave} achieves a new maximum value.

If we denote by $F_*^u: [0, 1]^2 \rightarrow [0, 1]$ the distribution function of Σ_*^u , $*$ = $\rho, \rho a$, given by

$$F_*^u(c, d) = \Sigma_*^u([0, c] \times [0, d])$$

then weak* convergence of Σ_*^u to the Lebesgue measure is equivalent to convergence of $F_*^u(c, d)$ to cd for all $(c, d) \in [0, 1]^2$ as $N \rightarrow \infty$. We remark that convergence of RSD_*^u to 0 is equivalent to

$$F_*^u(c, d) \rightarrow cd, \quad (c, d) = \left(\frac{i}{200}, \frac{j}{200} \right), \quad i, j = 0, \dots, 200.$$

Such convergence of distribution functions is known in statistics as Kolmogorov-Smirnov test [Smi39].

Finally let us mention that we have also performed similar numerics, such as the Kolmogorov-Smirnov test, for the dissipative family and the results are similar. It is more difficult to compare Σ^{SRB} and $\Sigma_{\rho a}^u$ in this case because the SRB measure is not Lebesgue. The difficulty comes from the fact that Σ^{SRB} is defined by (3.7) using the slice S of thickness $\Delta y = 10^{-2}$. In conservative case the value of Δy is irrelevant, but in the dissipative case the restriction of the SRB measure to the slice is no longer a product measure. Hence we also need to let $\Delta y \rightarrow 0$ in order to approximate the conditional measure on \mathbb{T}^2 . The additional parameter Δy makes numerics even more involved and we did not fully pursue it.

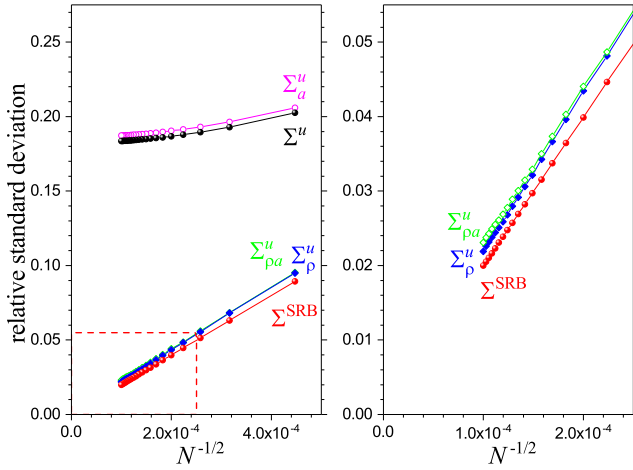


FIGURE 3.9. Relative standard deviations for $f_{C,\varepsilon=0.1}$ point distributions calculated for N between 5 to 100 million. The zoom-in on the right shows that both SRB measure and u measure (when properly weighted) converge to uniform distributions approximately as $N^{-1/2}$.

Acknowledgments. A.G. would like to thank Yakov Pesin who introduced him to questions in the spirit of our Conjecture 1.3 in his 2004 dynamics course. Also A.G. would like to thank Aleksey Gogolev who performed initial numerical experiments and created the first set of beautiful pictures back in 2008. During final stages of preparation of this paper discussions with Federico Rodriguez Hertz were very useful. We would like to acknowledge helpful feedback from Dmitry Dolgopyat, Yi Shi and Rafael Potrie. We also acknowledge helpful comments provided by the referee.

A.G. was partially supported by the NSF grant DMS-1204943. I.M. and A.N.K. gratefully acknowledge NSF support (Award No. DMR-1410514).

References

- [BDU02] Bonatti, C., Díaz, L., Ures, R. *Minimality of strong stable and unstable foliations for partially hyperbolic diffeomorphisms*. J. Inst. Math. Jussieu 1 (2002), no. 4, 513–541.
- [BDV00] Bonatti, C., Díaz, L., Viana, M. *Dynamics beyond uniform hyperbolicity. A global geometric and probabilistic perspective*. Encyclopaedia of Mathematical Sciences, 102. Mathematical Physics, III. Springer-Verlag, Berlin, 2005. xviii+384 pp.
- [BV00] Bonatti, C., Viana, M. *SRB measures for partially hyperbolic systems whose central direction is mostly contracting*. Israel J. Math. 115 (2000), 157–193.
- [BM58] Box, G.E.P, Muller, M.E. *A note on the generation of random normal deviates*. Annals Math. Stat. 29 (1958), 610–611.
- [BP74] Brin, M., Pesin, Ya., *Partially hyperbolic dynamical systems*. Izv. Akad. Nauk SSSR Ser. Mat. 38 (1974), 170–212.
- [CP15] Crovisier, S., Potrie, R. *Introduction to partially hyperbolic dynamics*. Lecture notes for a mini-course in School and Conference in Dynamical Systems, ICTP, Trieste.
- [Dol01] Dolgopyat, D. *Lectures on u -Gibbs states*, Lecture Notes, Conference on Partially Hyperbolic Systems (Northwestern University, 2001).
- [Dol04a] Dolgopyat, D. *Limit theorems for partially hyperbolic systems*. Trans. Amer. Math. Soc. 356 (2004), no. 4, 1637–1689.
- [Dol04b] Dolgopyat, D. *On differentiability of SRB states for partially hyperbolic systems*. Invent. Math. 155 (2004), no. 2, 389–449.
- [RGZ17] Ren, Y., Gan, S., Zhang, P. *Accessibility and homology bounded strong unstable foliation for Anosov diffeomorphisms on 3-torus*. Acta Math. Sin. (Engl. Ser.) 33 (2017), no. 1, 71–76.
- [Gog08] Gogolev, A. *Smooth conjugacy of Anosov diffeomorphisms on higher-dimensional tori*. J. Mod. Dyn. 2 (2008), no. 4, 645–700.
- [GG08] Gogolev, A., Guysinsky, M. *C^1 -differentiable conjugacy of Anosov diffeomorphisms on three dimensional torus*. Discrete Contin. Dyn. Syst. 22 (2008), no. 1-2, 183–200.
- [HPS77] Hirsch M., Pugh C., Shub M. *Invariant manifolds*. Lecture Notes in Math., 583, Springer-Verlag, (1977).
- [Jia12] Jiang, M. *Differentiating potential functions of SRB measures on hyperbolic attractors*. Ergodic Theory Dynam. Systems 32 (2012), no. 4, 1350–1369.
- [Mañ78] Mañé, R. *Contributions to the stability conjecture*, Topology 17 (1978), 383–396.
- [PM88] Park, S.K., Miller, K.W. *Random number generators: good ones are hard to find*. Communications of the ACM, 31 (1988), 1192–1201.
- [Pes04] Pesin, Ya. *Lectures on partial hyperbolicity and stable ergodicity*. Zurich Lectures in Advanced Mathematics. European Mathematical Society (EMS), Zürich, 2004. vi+122 pp.
- [PS83] Pesin, Ya., Sinai, Ya. *Gibbs measures for partially hyperbolic attractors*. Ergodic Theory Dynam. Systems 2 (1982), no. 3-4, 417–438 (1983).
- [Pot14] Potrie, R. *A few remarks on partially hyperbolic diffeomorphisms of T^3 isotopic to Anosov*. J. Dynam. Differential Equations 26 (2014), no. 3, 805–815.
- [PS06] Pujals, E., Sambarino, M. *A sufficient condition for robustly minimal foliations*. Ergodic Theory Dynam. Systems 26 (2006), no. 1, 281–289.
- [Rue97] Ruelle, D. *Differentiation of SRB states*. Comm. Math. Phys. 187 (1997), no. 1, 227–241.
- [Rue98] Ruelle, D. *Nonequilibrium statistical mechanics near equilibrium: computing higher-order terms*. Nonlinearity 11 (1998), no. 1, 5–18.
- [Smi39] Smirnov, N. *On the estimation of the discrepancy between empirical curves of distribution for two independent samples*. Bull. Math. Univ. Moscou 2, (1939). no. 2, 16 pp.

- [Yan16] Yang, J. *Entropy along expanding foliations*.
`arXiv:1601.05504v1`
- [You86] Young, L.-S. *Stochastic stability of hyperbolic attractors*.
Ergodic Theory Dynam. Systems 6 (1986), no. 2, 311–319.
- [You02] Young, L.-S. *What are SRB measures, and which dynamical systems have them? Dedicated to David Ruelle and Yasha Sinai on the occasion of their 65th birthdays*. J. Statist. Phys. 108 (2002), no. 5-6, 733–754.

Andrey Gogolev,⁷
 Mathematical Sciences,
 SUNY Binghamton, N.Y., 13902, USA
agogolev@math.binghamton.edu

Aleksey Kolmogorov,
 Physics Department,
 SUNY Binghamton, N.Y., 13902, USA
kolmogorov@binghamton.edu

Itai Maimon
 Mathematics and Physics
 SUNY Binghamton, N.Y., 13902, USA
imaimon1@binghamton.edu

⁷Currently at Department of Mathematics, Ohio State University, Columbus OH.